SEISMOLOGY AND GEOMAGNETISM

The Seismology and Geomagnetism Group is engaged in a variety of studies in both seismology, and electromagnetic induction. The current research activities have a common thread of using wave propagation processes to study the nature of the Earth. The work combines field observations, theoretical work, computer modelling and extensive data analysis to exploit the favourable geographic location of Australia for seismic and electromagnetic studies.

SEISMOLOGY

The major area of research in Seismology is the investigation of the internal structure of the Earth using the seismic waves generated by both natural and man-made sources as probes. Much of the work is directed towards improving our understanding of the three-dimensional variation in the seismic properties of the Earth's interior, and involves a number of activities including observation, interpretation and theoretical developments.

Dr A. Gorbatov whose specialisation is seismic tomography joined us in April and has provided valuable support to the field program. Dr A. Reading arrived in December and will take a major role in the future observational work.

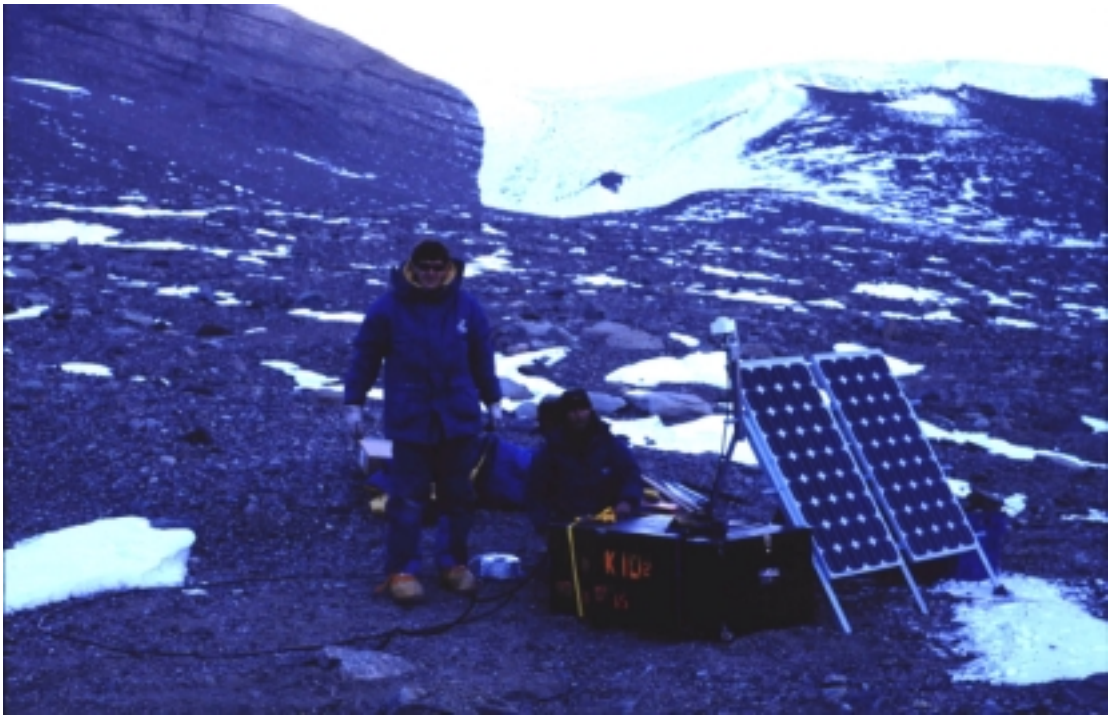

Figure 1: S. Sirotjuk at the seismic station in the Lower Wright Valley (-77.45 S, 162.59 E) in the Transantarctic Mountains with the instrument package and solar panel assembly.

A wide variety of techniques have been applied to the study of the variations in mantle structure beneath the Australasian region, and it has now been possible to develop a three-dimensional picture of the variation of seismic attenuation beneath the continent which exploits the coverage by refracted body waves. Research continues into improved methods for surface wave tomography with the development of better methods for assessing the zone of influence around the propagation path and non-linear inversion to extract multi-mode dispersion. This work and a number of other studies exploit the neighbourhood algorithm devised by Dr M. Sambridge, and in particular the ease with which it can be adapted to new problems.

The group maintains an active observational program based on the use of arrays of portable recorders, with deployments this year in the Transantarctic mountains and in western Australia.

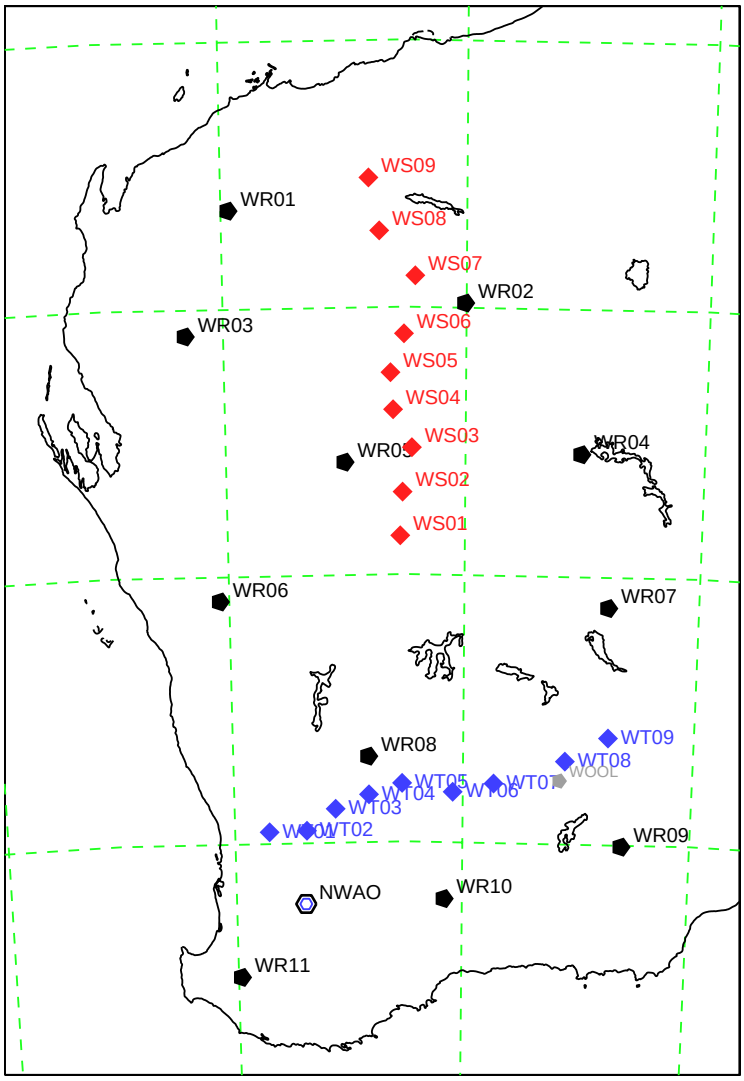

Figure 2: Configuration of the broadband stations in the West Australian Craton experiment. The WR sites have a long term deployment with CMG3-ESP seismometers (STS-2 at WR5). The remaining stations have CMG-40T seismometers, the WS sites were occupied from July to October, and the WT sites from October.

From November 1999 to February 2000, a joint experiment was carried out with the Institute of Geological and Nuclear Sciences of New Zealand in the Transantarctic Mountains. A set of ten broadband stations were successfully operated using a combination of ANSIR and RSES equipment with logistic support, mostly by helicopter, from Antarctic New Zealand out of Scott Base. The stations were operated with solar power through the long days of the Antarctic summer (Figure 1), using a design developed in RSES for support of GPS stations. Both S. Sirotjuk and T. Percival were involved with the fieldwork in Antarctica which has returned good quality data, with a good distribution of teleseismic events during the period of the deployment.

From July the observational focus moved to the Archaean cratons of West Australia. A major experiment combines most of the RSES broadband equipment with the Orion recorders from the ANSIR national facility. A broadly distributed network of stations (WR sites – Figure 2) will be in place for at least six months at each site, and this is complemented by linear arrays (WS, WT with a recording span of at least twelve weeks). The broad network is designed to

provide suitable coverage for surface wave tomography. The linear profiles have been chosen to cross major features in this Precambrian region with an emphasis on receiver function studies. The WS line crosses from the Pilbara craton through the Capricorn orogen to the Yilgarn craton. The WT line crosses the three major divisions of the Yilgarn block and links from the Mundaring observatory behind Perth to the goldfields region near Kalgoorlie.

The program of upgrade at the Warramunga Array to meet the operational requirements of the Comprehensive Nuclear-Test-Ban Treaty (CTBT) is now largely complete. The new infrasound array required the installation of rather complex wind-reducing filters, and this proved to be a considerable challenge. The entire configuration was completed at the end of September but infrasound data had been transmitted to the International Data Centre from July, once the basic sensors were in place. J. Grant and his team at Tennant Creek are to be congratulated on the successful completion of two major facilities – the upgraded twenty four element seismic array and the new eight element infrasound array. Certification of compliance to treaty standards is expected once data authentication facilities are fully installed.

Extending surface wave tomography

K. Yoshizawa, Y. Hiyoshi and B.L.N. Kennett

The influence zone about a surface wave path.

An approximate description of the zone of influence around the propagation path for a surface wave is provided by the Fresnel-zone for the frequency of interest. A new technique called "Fresnel-area ray tracing" (FRT) for estimating this zone around the ray path, has been developed by combining elements of two standard ray tracing techniques, "kinematic ray tracing" (KRT) and "dynamic ray tracing"(DRT).

To obtain the exact Fresnel area in a laterally heterogeneous structure, we would need to solve a large number of KRT equations. In contrast, the FRT approach requires just a few ray tracing calculations. In the first step, the trajectory of the surface-wave is computed by solving the KRT system for the phase-velocity distribution at the required frequency. In the next step, the behaviour of rays in the zone surrounding the KRT path are calculated by solving the DRT system twice: once from source to receiver and once more from receiver to source along the same trajectory. Finally, combining the solutions of these ray tracing systems, Fresnel area around a central ray can be estimated.

Examples of rays for Rayleigh waves are shown in Figure 3. These rays have been traced on a phase velocity map at 40 second periods derived from the three-dimensional model for structure around the Australian Continent model developed by Debayle and Kennett (2000). In the upper panel, off-great-circle propagation and multi-path effects are apparent for some regions of the model. Approximate Fresnel areas for ray paths from three events to the CAN station in southeastern Australia are shown in the lower panel. The radius of the Fresnel zone depends mainly on the path length and the velocity gradient transverse to the central ray. The areas which may affect the actual wavefield can be recognised by using these finite-width ray plots.

The method of FRT is simple and computationally effective and allow us to extend current methods of surface-wave analysis which have commonly been based on geometrical ray theory and on the approximation of great-circle propagation. We are now able to treat ray paths with "finite-width" as well as the deviations in propagation from the great-circle induced by strong heterogeneity.

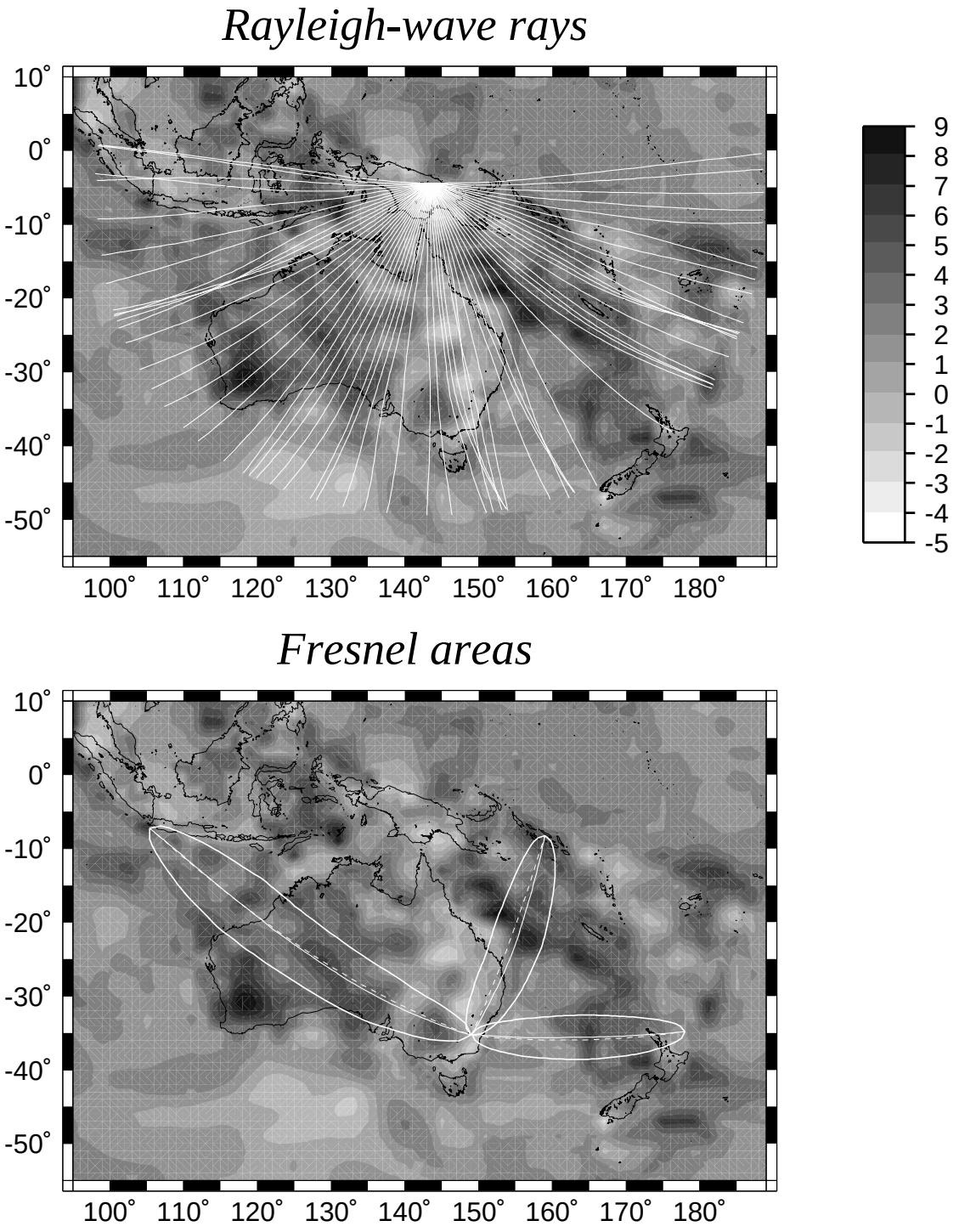

Figure 3: Rayleigh wave rays (top) and Fresnel areas (bottom) superimposed on a 40 second phase velocity map. Fresnel areas are plotted with solid elliptical lines, central rays with solid lines in the ellipses and great-circles with dashed lines. The greytone scale indicates the deviation in percent from the reference phase velocity of 3.93 km/s

Multi-mode waveform inversion using a Neighbourhood Algorithm.

The first step in surface wave tomography is to invert for a one-dimensional model for which calculated waveforms match suitably filtered observations. This process depends on a knowledge of the source mechanism and with linearised inversion can be quite sensitive to the starting model with consequent ambiguities in the model. There are therefore advantages in

adopting a non-linear approach which does not require calculation of derivatives. This then allows considerable flexibility in the measures of fit between observed and synthetic seismograms. The non-linear inversion has been achieved using a neighbourhood algorithm (NA) exploiting multi-mode synthetic calculations, with the advantage that there is substantial exploration of parameter space.

With different approaches to the parameterisation of the shear velocity profile, we can find models with significant differences in velocity variation with depth that provide similar levels of fit to the observed waveforms. Although the models differ, the calculated phase velocity dispersion with frequency for the first few modes of the surface waves are very close indeed. We therefore regard the one-dimensional models derived from the multi-mode waveform inversion as providing an implicit description of the path-average dispersion for each of the modes. If the perturbations from the reference model are weak it may be justified to interpret the one-dimensional models themselves as an average along the path, but the inversion does not depend on this assumption.

The inversion procedure samples a significant number of models. We select the one-dimensional wavespeed model that achieves minimum misfit. Phase velocities for each mode-branch are then calculated from the model parameters with the minimum misfit. An example of the NA waveform inversion for a synthetic case is shown in Figure 4: 3000 S-velocity models generated during the exploration of parameter space are displayed with a grey tone that becomes progressively darker as the misfit decreases. The models with lower misfit concentrate around the true model, and the phase velocities for a number of modes are recovered very well.

The NA approach has proved to be very efficient for finding the best-fit model that gives a good match between observed and synthetic waveforms and so provides good phase-velocity recovery. Good results have been achieved with both Rayleigh and Love wave inversions for a range of different paths.

The multi-mode phase velocities measured using this approach can be used to retrieve two-dimensional phase velocity maps as a function of frequency, which provide strong constraints on three-dimensional Earth models. Because we use the one-dimensional models as a summary of the average phase velocity dispersion along the path we do not need to make any assumptions about the nature of anisotropy. We can employ simple isotropic models and determine anisotropic properties from the angular and depth dependence of the two-dimensional phase velocity distributions.

Polarisation anisotropy for Australian paths.

The studies of Rayleigh wave propagation across Australia have revealed very strong contrasts in seismic wavespeed in the mantle beneath the Phanerozoic zone in the east and the Precambrian regions in the west and centre. Simultaneous analysis of the waveforms of Rayleigh and Love waves indicate that there is a need to introduce polarisation anisotropy which varies with depth. Different velocity models are needed for vertically polarised S waves (SV) and horizontally polarised SH waves. The SV model is derived largely from the Rayleigh wave data and the SH models from Love waves. Significant polarisation anisotropy exists for paths which cross the zone of fast SV wavespeeds in western and central Australia, but the differences between SV and SH velocities is less pronounced under eastern Australia.

It is often difficult to achieve a comparable fit to the waveforms of both Rayleigh and Love in a simultaneous inversion. This arises because of the larger sensitivity of the Love inversion to starting model. We have found that when a transversely isotropic model is used in linearised inversion that the general character of the polarisation anisotropy is similar from different starting models when convergence is achieved, but the level of differences between the SV and SH waveforms can depend on the style of parameterisation. Even with a robust approach such as the Cara-Leveque method it may not be possible to find a satisfactory SH wave model for a range of paths using a single starting model.

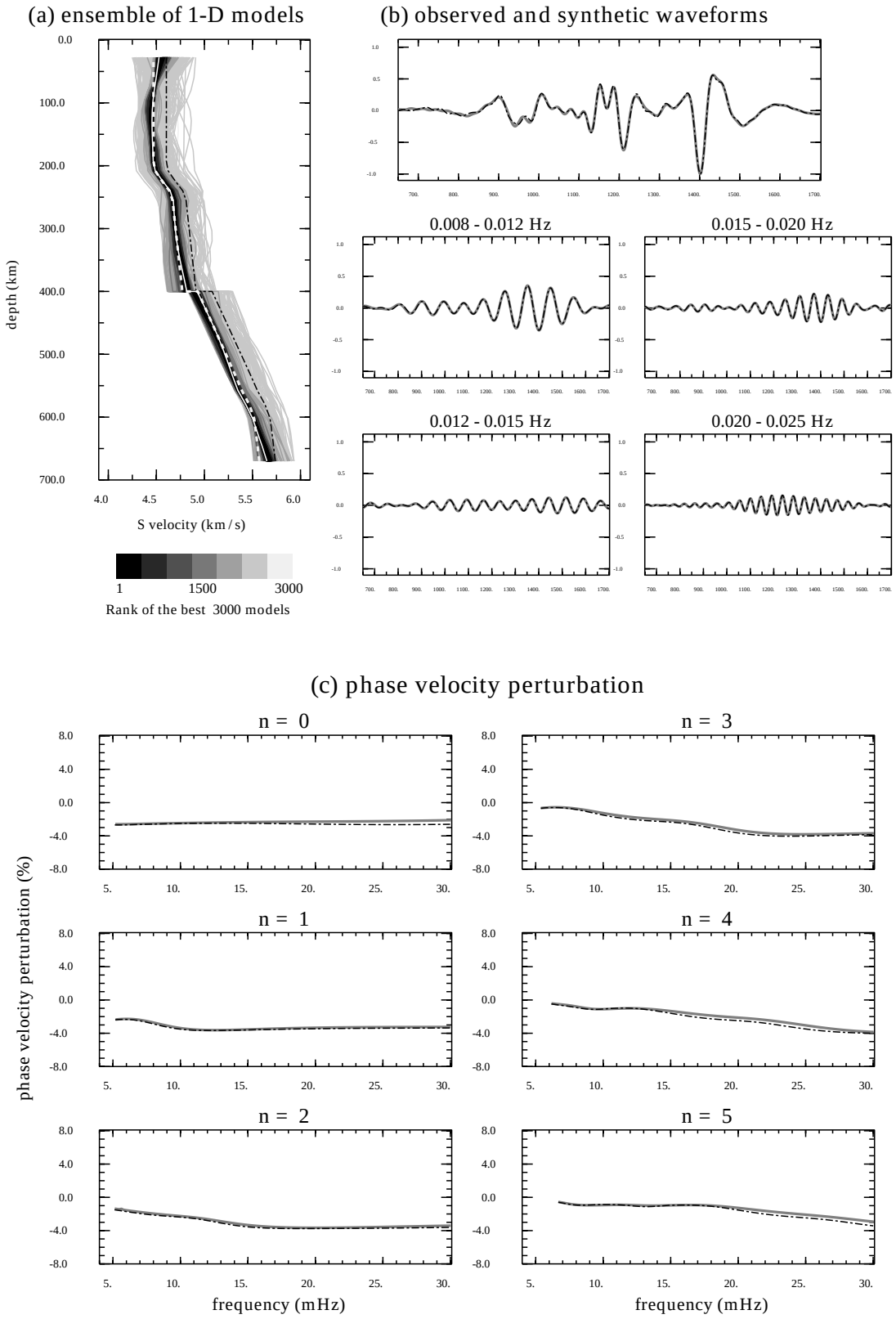

Figure 4: (a) Density plot of all 3000 S-velocity models generated by a NA technique for Rayleigh wave inversion. The white solid line is the best-fit model, the white dotted line is the true model, the black chain-dotted line is the reference model used to initiate the inversion. (b) Seismograms calculated from the best-fit model (grey) and from a true model (black chain-dotted). The original seismograms are displayed at the top and filtered seismograms in four frequency ranges are shown at the bottom. (c) Phase velocity perturbation of the first six mode-branches estimated from the best-fit model (grey) and from a true model (black chain-dotted).

Attenuation of seismic body waves in the Australian region

H-X. Cheng and B.L.N. Kennett

The wide range of body wave observations at distances up to 40° recorded at the SKIPPY and KIMBA experiments provide good coverage of the upper mantle, particularly under northern Australia. The differential attenuation between P and S waves can be extracted from the spectral ratio as a function of frequency. For frequencies less than 1 Hz the effect of frequency dependence is weak and a robust estimate of the differential attenuation between P and S phases can be extracted from the slope of the logarithmic spectral ratio in terms of the parameter. The use of broad-band seismic observations (up to 6 Hz) allows the examination the frequency dependence of attenuation. A simple model of a power law dependence on frequency provides a reasonable good description of the observations. A set of differential attenuation estimates have been made over 6 bands in frequency (related by the Golden section) with the aim of characterising the variation with frequency.

The extensive set of differential attenuation measurements from over 1500 paths can be exploited to invert for attenuation structure if the velocity structure is known. We are able to make use of the set of fifteen models for different azimuthal corridors across the continent which were based on the interpretation of stacked sections of body wave arrivals. A similar approach of data organisation into azimuthal corridors was used for the inversion of differential attenuation data to produce a set of one-dimensional Q profiles for 5 or 6 layer models. The inversion of the variation in differential attenuation with range was carried out using a neighbourhood algorithm (NA) approach for parameter space exploration, which allows an assessment of the properties of a group of models with good fit to the data as well as just finding the best fitting model.

A three-dimensional Q model was then constructed by combining these one-dimensional Q profiles weighted by the ray density in a cellular model. We used 2x2 degree cells in a 6 layer model over the region 0–46°S, 100–170°E and extracted an estimate of the loss factor Q^{-1} in a particular cell by averaging the one-dimensional Q^{-1} profiles, which overlap in this cell, weighted by the vertical and horizontal raypath density functions. Figure 5 displays a set of map views of the pseudo three-dimensional Q structure obtained using this procedure. Images are shown for the layers 0–75.5 km, 77.5–120 km, 120–210 km, 210–410 km, 410–660 km, 660+ km. These pseudo three-dimensional Q images present the first representation of the three-dimensional spatial variation of attenuation in the mantle for the Australian region. The dominant result is that Q tends to first to decrease with increasing depth and then increase; the attenuation of seismic waves is weak in the shallow part (< 120 km) of the Earth. There is also a strong contrast in attenuation between the east of Australia with lower Q and the centre and west with higher Q, particularly in the depth range from 77.5–210 km. This pattern shows a strong correlation with the results for shear wave speed structure. Fast S wavespeeds correspond to low attenuation (high Q), whereas lowered S wavespeeds are found in the regions with high attenuation (low Q).

The results in Figure 5 are based on the differential attenuation measurements for a frequency around 0.6 Hz. We are also able to use the broad band results to examine the frequency dependence of attenuation. Forward modelling indicates that over the frequency range up to 6 Hz the influence of dispersion is small, and so we are able to work with a single set of velocity models.

From the measurements over the set of six frequency bands we are able to assemble estimates of the variation of the differential attenuation as a function of both frequency and distance for each azimuthal corridor. With the assumption of a power law variation in Q as a function of frequency f, ($Q = Q_0 f^{\alpha}$) a NA inversion was again used to derive a one-dimensional profile for Q_0 and the exponent α. The set of one-dimensional models could then be used, as before, to derive an approximate three-dimensional model. The variation of the exponent α is illustrated in Figure 6, and shows strong depth dependence as well as the lateral variation. In general, the exponent α is small in the shallow part of the Earth, and then increases with depth to

its largest value in the layer, between 210–410 km, and then decreases in the lower mantle. The variation in α is from 0.02 to 0.98, but is generally smaller than 0.5.

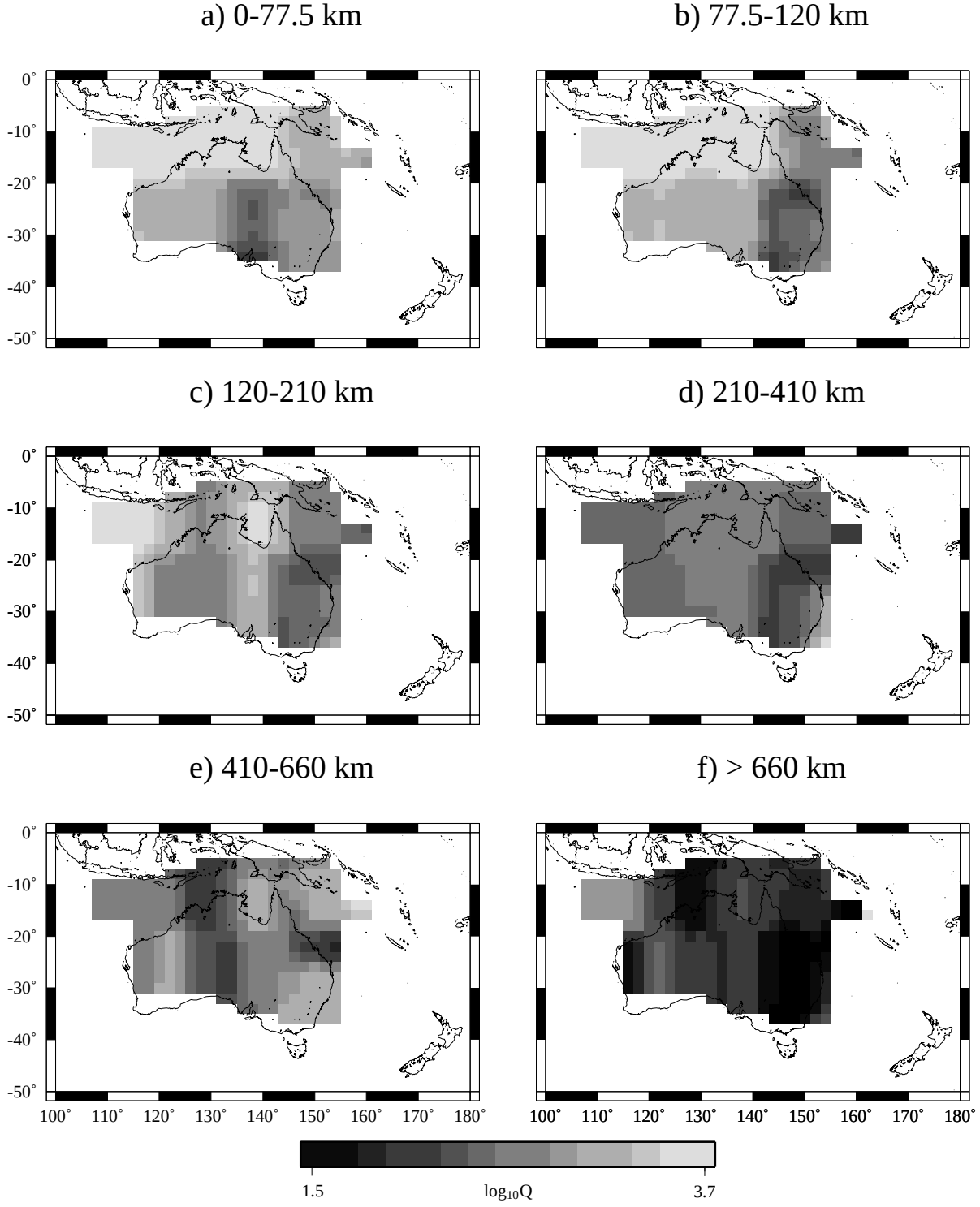

Figure 5: Model of the three-dimensional variation in Q in the mantle beneath Australia derived from measurements of differential attenuation between P and S waves via a set of one-dimensional profiles for different azimuthal corridors.

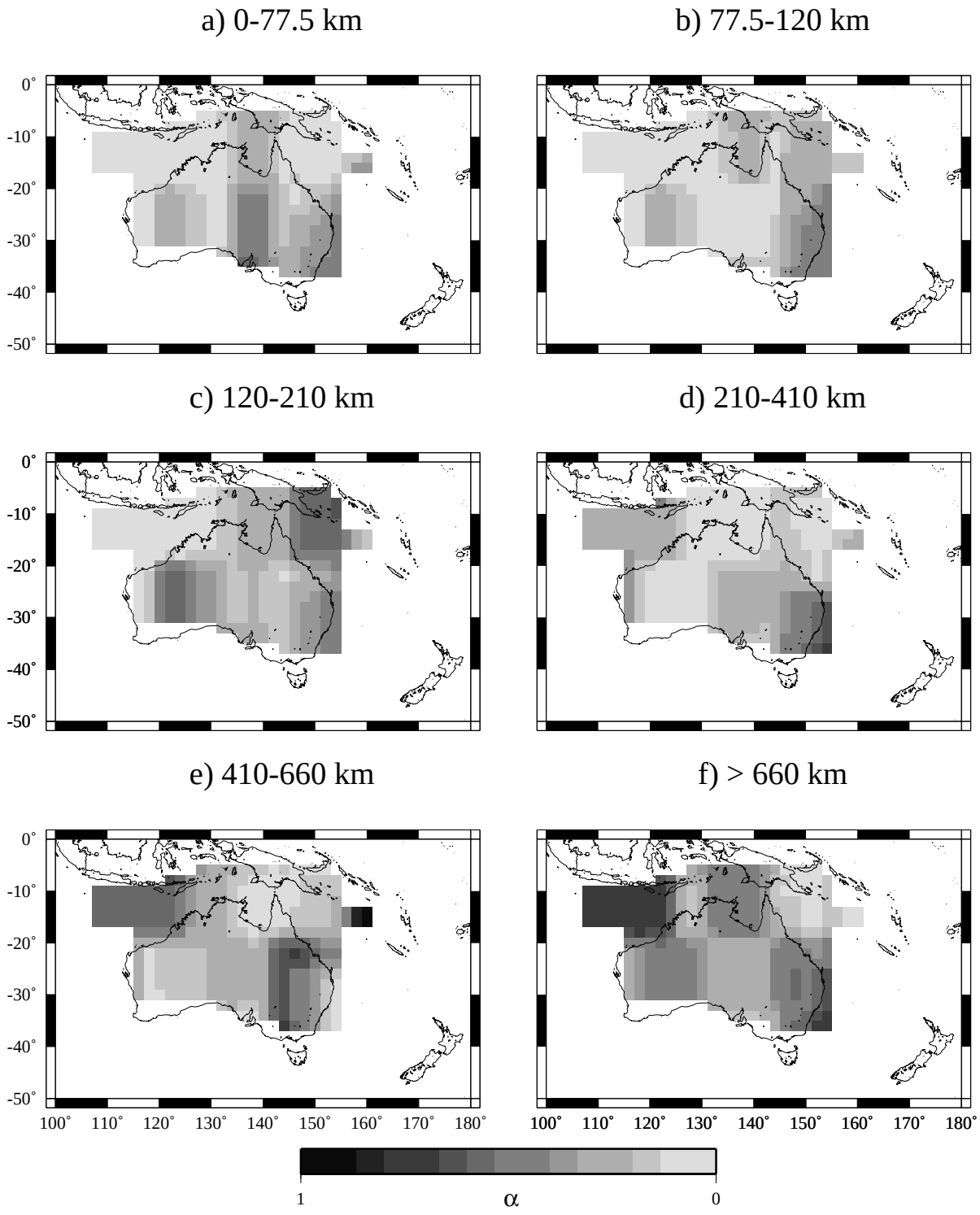

Figure 6: Model of the three-dimensional variation in the exponent α of power law dependence of Q in the mantle beneath Australia derived from differential attenuation measurements or frequencies up to 6 Hz.

Seismogram inversion using a Neighbourhood Algorithm - application to source inversion and receiver functions

K. Marson-Pidgeon, B.L.N. Kennett and M. Sambridge

The inversion routine for obtaining source parameters described in last year's annual report has been applied to a number of moderate magnitude events. Teleseismic waveforms are inverted for source depth, time function and mechanism (including an isotropic component), and use a neighbourhood algorithm to search the parameter space.

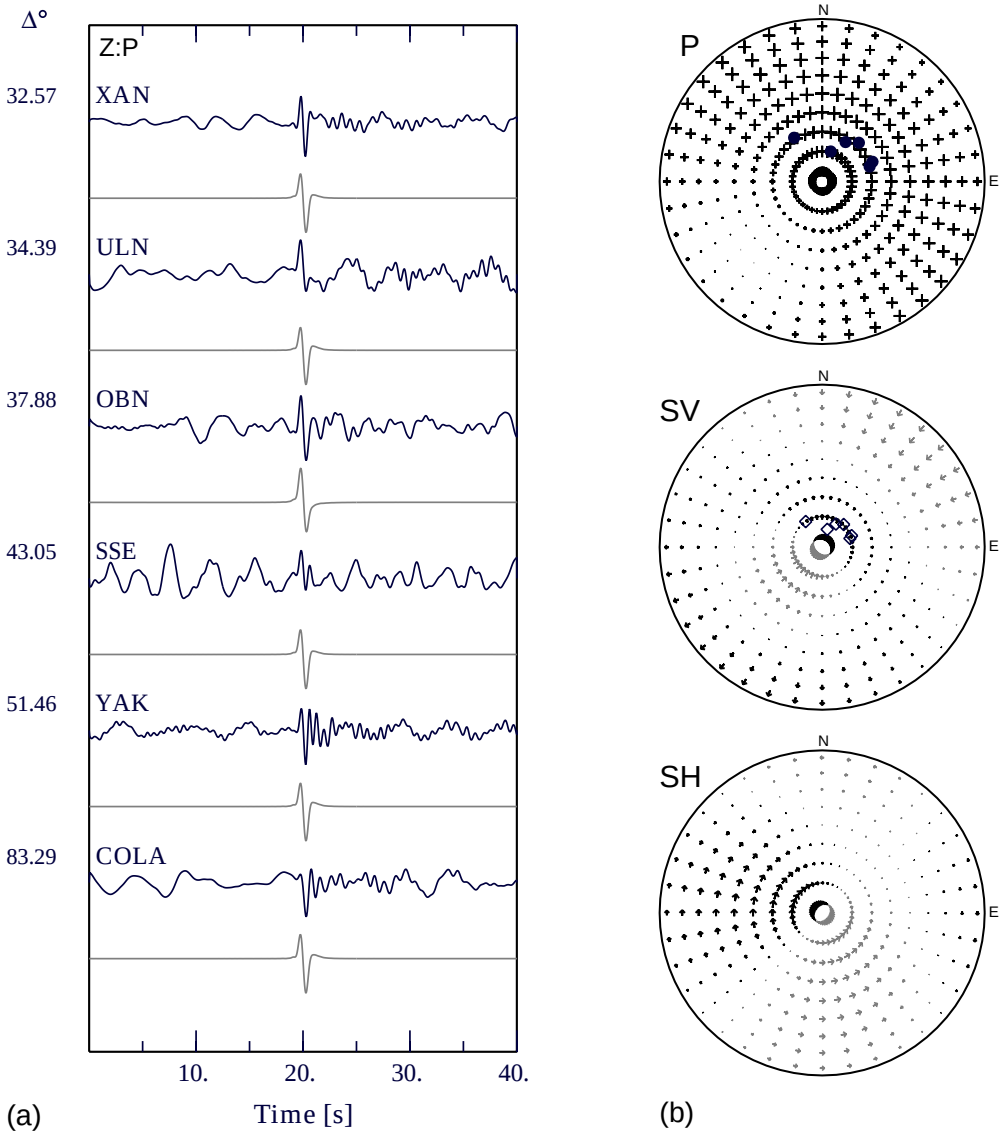

Figure 7: Results of a waveform inversion using just P waves for the 11 May 1998 Indian nuclear test. (a) Comparison between the observed (black traces) and predicted (grey traces) seismograms for the vertical component of P. The epicentral distances are displayed on the left, along with the station names. (b) Predicted P, SV and SH source radiation patterns obtained from the inversion.

One important application of this method is discrimination between small to moderate magnitude earthquakes and nuclear explosions. As a test of the discrimination capabilities of the inversion routine we apply it to a known nuclear explosion; the Indian nuclear test of 11 May

1998. We obtain a best fitting source depth of 0.6 km, which provides a good fit to the observed P wave seismograms (Figure 7). Based on the depth estimate alone, we have grounds to suspect this event of being man made. The result of the inversion indicates a large isotropic moment (at least 50% of the total moment), Although the source mechanism estimate we obtain is not wholly explosive (Figure 7), our results with only a few stations provide strong evidence to suspect this event of being a nuclear test and therefore requiring further investigation.

The inversion routine has also been applied to five earthquakes of moderate magnitude (mb ranging from 5.6 to 5.8). One of the earthquakes occurred off the east coast of Honshu, Japan (see last year's annual report), and the other four were all in continental regions. Inversion using a standard velocity model worked well for the two earthquakes, which occurred in southern Xinjiang, China, and Kyrgyzstan. The depth and mechanism estimates obtained from these events were close to the published Centroid Moment Tensor (CMT) information. For two strike-slip events in Turkey and on the India-Bangladesh border we were not able to obtain well-constrained solutions. Such inversions would be improved by the inclusion of regional data. In the case of the India-Bangladesh border event, the location in a region of strong crustal heterogeneity means that the simple modelling scheme is unable to obtain a reliable inversion result. We do, however, obtain depth estimates close to the CMT depth estimate for both events, which is encouraging and indicates that our method is able to obtain accurate depth estimates even for problematic events.

The neighbourhood algorithm is also being applied to receiver function inversion for crustal structure. So far synthetic testing has been undertaken, but we hope to apply it to observed data in the near future. Since we are using a derivative-free inversion method we are able to investigate various misfit measures. We have tested L2, L2.5 and L3 norm misfit measures for various crustal structures, but it is not yet obvious which is the best to use in all cases. Each misfit measure tends to emphasise certain arrivals, but not others. More stable results are obtained when the Vp/Vs ratio in each layer is held fixed in the inversion. The best recovery of the input model has been obtained by using events from different distances (and therefore different slownesses) recorded at the same station. Each corresponding receiver function is then modelled separately (with the appropriate slowness) and their misfits are simply summed. This results in better constrained solutions since more information is being exploited in the inversion.

Assessment of uncertainty in model parameters

M. Sambridge and C. Farmer

The neighbourhood algorithm (NA) (developed at RSES, and reported on in previous years) is a direct search method for non-linear inversion. In the past few years, students and staff in Seismology have been using it to locate earthquakes, determine source mechanisms, as well as estimate attenuation and velocity structure in the upper mantle beneath Australia. In all of these studies we not only look for a model that fits the data best (in some sense), but also the range of parameters that satisfy the data. In non-linear problems the latter is more difficult to determine.

Over the past year, the NA has been applied to the problem of estimating the uncertainty in model parameters using a direct (non-Bayesian) approach. It was found that by choosing appropriate measures of data fit and then specifying an acceptable level, one could make the NA 'map out' the region (or regions) of parameter space containing acceptable models. Figure 8 shows an example where receiver functions are used as the data and the parameters describe the shear velocity as a function of depth in the Earth's crust. The ensemble of Earth models found by the NA is shown projected onto four pairs of velocity model parameters. The dark regions correspond to the data-acceptable models located using the new approach. Notice that they define irregular shaped regions and are far from elliptical (as would be predicted by linear theory). The size and shape of these regions indicates the uncertainty and trade-offs in the model parameters.

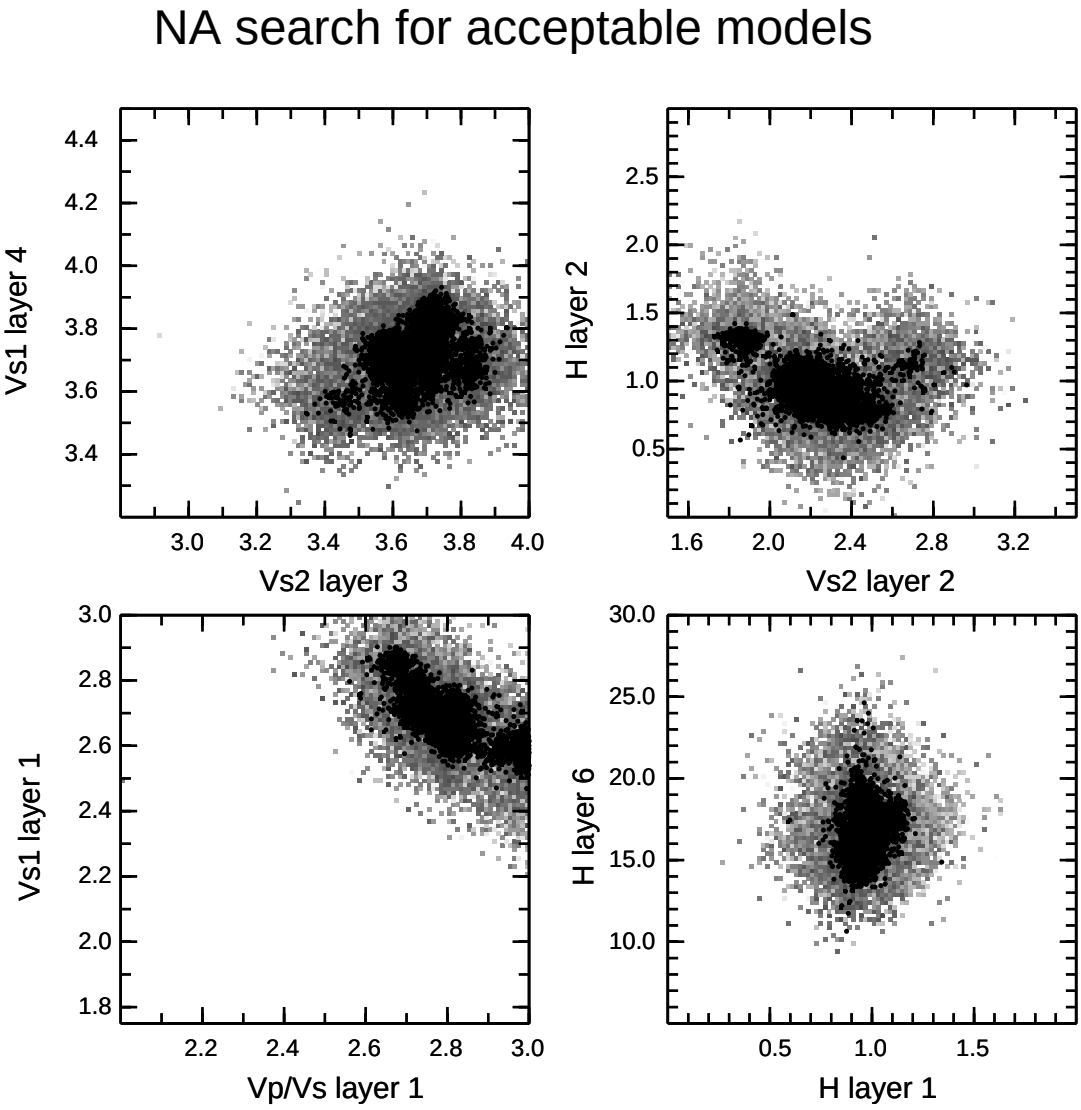

Figure 8: An ensemble of Earth models, found by the neighbourhood algorithm when trying to fit seismic receiver function data. The complete ensemble of velocity models has been projected onto four pairs of axes. The black regions correspond to models which fit the data to an acceptable level, given noise in the data. The shape of each acceptable region reflects uncertainty in the parameters.

Earthquake location without an Earth model

T. Nicholson, M. Sambridge and O. Gudmundsson[1]

Traditionally hypocentre location methods have relied upon a model for the seismic velocity of the Earth. However, the direct use of a such velocity model may be unnecessary and may actually limit the accuracy of location procedures. Over the past thirty five years, a database of large, reliably located events has been built up from observations made by a global network of stations. We have used this database of previous events in a novel location procedure, which avoids the use of an explicit velocity model.

The standard location procedures compare the observed arrival times for a new event to predicted times using the travel times for different seismic phases derived from an earth model.

[1] Danish Lithosphere Center, Copenhagen, Denmark

In our approach, called the arrival pattern method, we compare these observations directly with the travel times for existing events from the database. The pattern of arrivals is used to provide a quantitative measure of the similarity between the new event and the previous events. For each previous event there is an "arrival pattern misfit" value defined at its location.

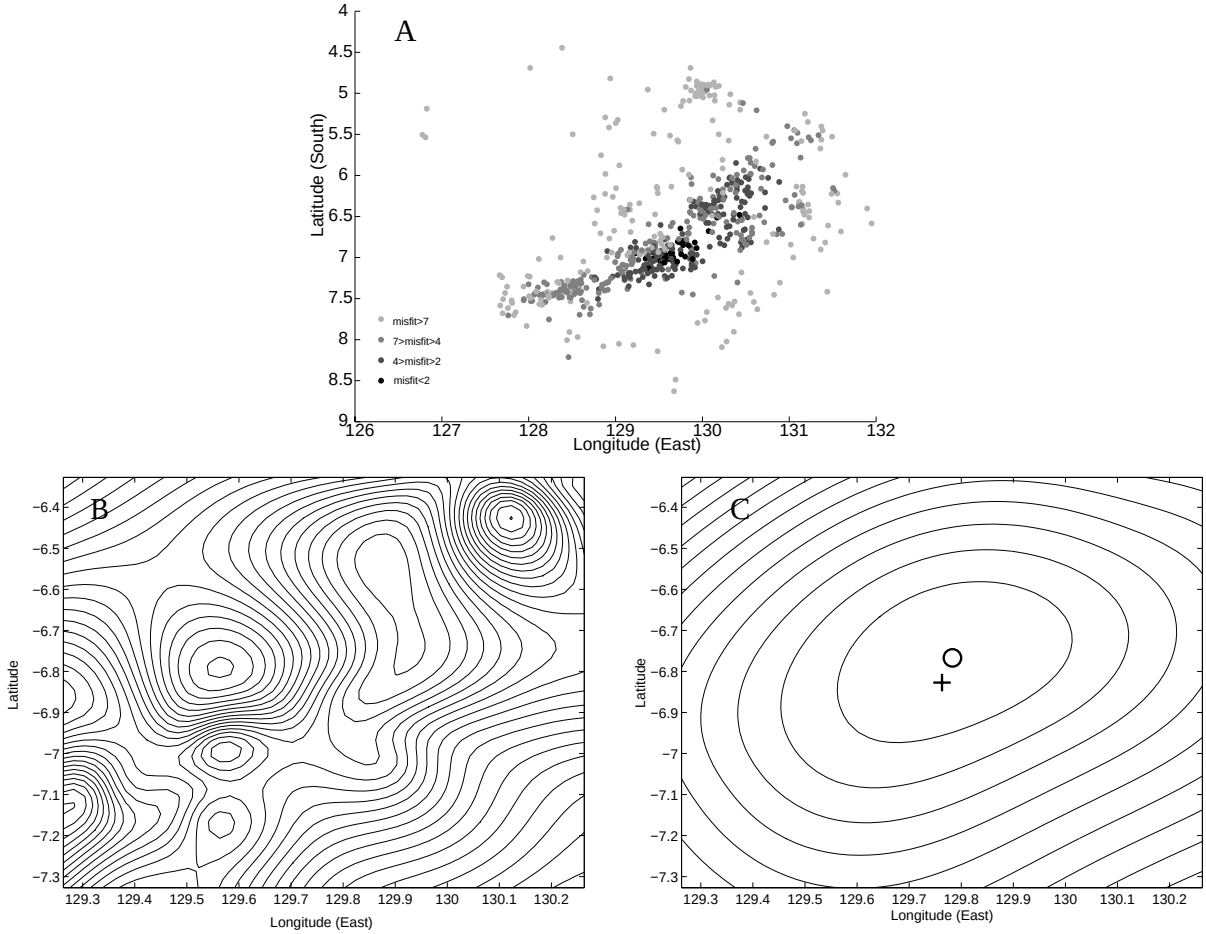

Figure 9: Arrival pattern misfit for an earthquake under the Banda Sea, Indonesia. (a) The misfit at the locations of nearby database events. (b) The misfit surface interpolated from the points in (a). (c) The misfit surface after smoothing with GCV has been applied. The circle is the location of the minimum misfit and the black cross is the EHB location.

The arrival pattern misfit is shown in Figure 9A for a new, magnitude 5.5 event in Indonesia compared to database events from the EHB catalogue, Engdahl *et al.*, *Bull. Seism. Soc. Am.*, **88**, 722–743. 1998. Each point in Figure 9A is a database event. The misfit is not known between the database events. However, we can use thin-plate spline interpolation to 'fill in the gaps' and this allows a contour diagram of misfit to be drawn, such as that shown in Figure 9B. Unfortunately, the observations for both the new and database events contain noise and, as a result, the misfit surface in Figure 9B has an undulating nature with several local minima and maxima. The situation can be improved by suitable smoothing of the arrival pattern misfit. We make use of a smoothing regime commonly used elsewhere, but rarely used in seismology, called generalised cross validation (GCV). GCV determines the degree of smoothing needed, based solely on the data, not on an arbitrary choice as is often required in smoothing techniques. An example of the misfit contours smoothed by GCV is shown in Figure 9C. The minimum of the smoothed misfit is called the arrival pattern hypocentre.

By using this approach we have been able to match the accuracy of even the best model based locations and as the database grows the accuracy of the arrival pattern method will continue to improve. A strength of the arrival pattern approach is that new database events may

be easily added and multiple databases can be used simultaneously, which gives an opportunity to account for the many scales of lateral heterogeneity that exist within the Earth.

P wave tomographic imaging of the southwest Pacific

A. Gorbatov and B.L.N. Kennett

Tomographic studies of the Earth structure provide important keys for understanding of tectonic processes and the control of natural resources. The quality and resolution of tomographic images depends on a number of factors, including the data density and the way in which the tomographic inversion is implemented. We seek a flexible representation of the features within the Earth and seismic ray propagation so that we can make as close an approach as possible to reality with available computational resources.

The quality of available data continues to improve as new arrival time observations are added from international and Australian studies and also earlier data is reprocessed to improve event locations. Increased data density in turn allows an improvement in the resolution of tomographic images.

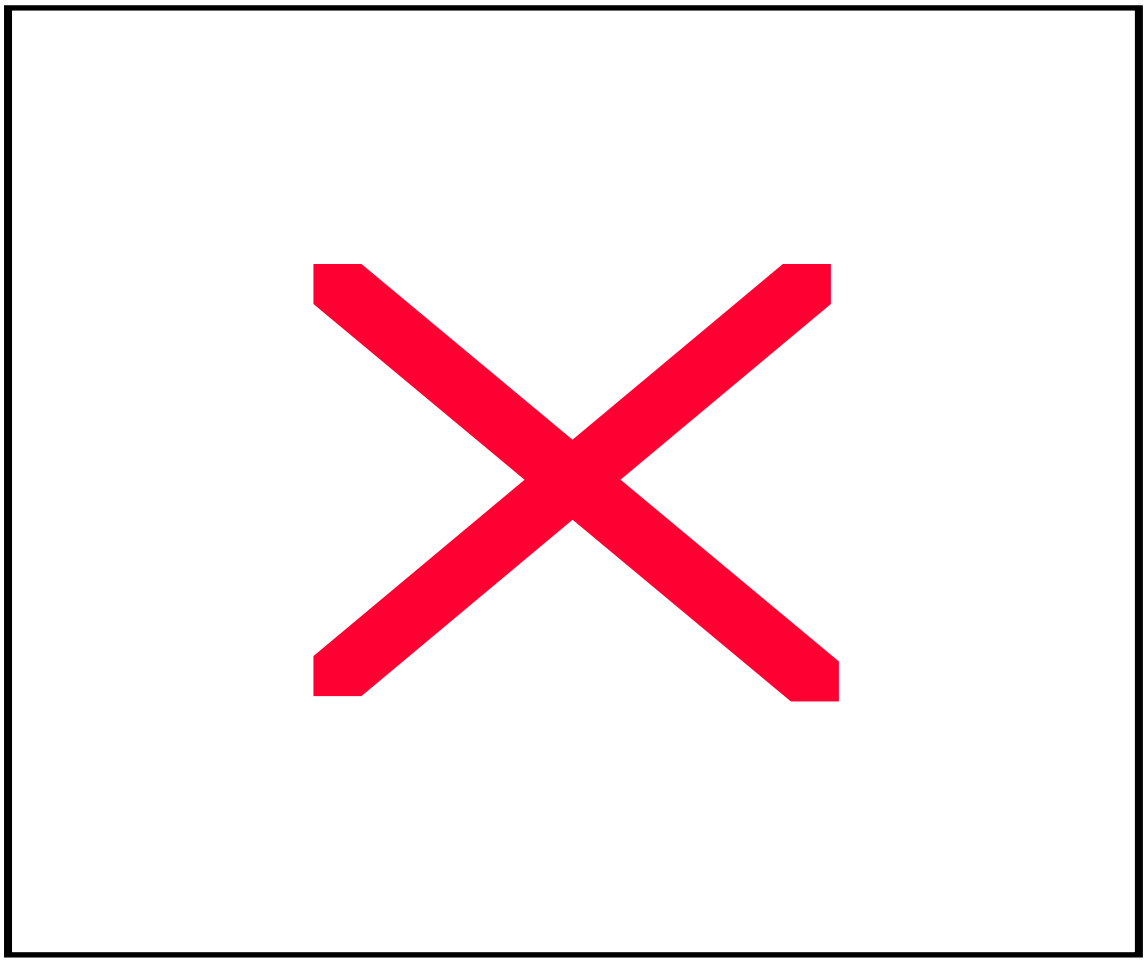

Figure 10: Cross sections through the P wave tomographic model for the Southwest Pacific showing the strong contrast between the fast Australian lithosphere and the low wavespeed zones flanking the narrow subduction zones.

However, even the new data catalogues have imperfections and the data density varies considerably from region to region, because the distribution of ray paths is controlled by

positions of available events and stations. In particular, there are strong contrasts in ray path coverage for Australia and its surrounding areas. Ray path density is high close to the subduction zones, but drops to low below Australia with concentration at a limited number of seismic stations. There is the additional complication that there can be considerable variations in the scale of wavespeed variation from a few tens to several hundred kilometres.

If we could adapt the parameterisation of the Earth model to the nature of the structures under study and the available data density, we should be able to significantly increase the resolution attainable of the inversion. However, we should avoid imposing too tight a set of *a priori* constraints on the results. We have, therefore, implemented a tomographic inversion with a parameterisation which has smaller cells near the Earth's surface and larger cells at depth with a scale length chosen to reflect the likely variations in the subduction zones of the southwestern Pacific. Blocks of 50 x 50 x 50 km have been used in the upper mantle, and the cell size is increased to 100 x 100 x 100 km blocks in the middle mantle.

In order to stabilise the inversion, several different approaches to model regularisation have been tested. Both first and second derivative smoothing kernels have been tested. We find that a second-derivative smoothing kernel is more useful for the inversion where strong, small-scale velocity gradients are present, such as in subduction zones, due to the less aggressive smoothing features.

A realistic ray propagation algorithm is important for mapping of fine scale structure, especially for subduction zones where lateral seismic velocity contrasts are strong and can have a strong influence on ray propagation. We have used an iterative development with a three-dimensional ray-tracing algorithm, which exploits the three-dimensional structures recovered during the course of the inversion. This refinement of the ray-path trajectories gives a significant improvement to the tomographic results, particularly through improving the contrast and visibility for small velocity structures.

Figure 10 illustrates the tomographic image for the southwestern Pacific region in which the subduction zones below New Caledonia, the Solomon Islands, and Papua New Guinea can clearly be seen through their contrast with their surroundings. The generally high seismic wavespeeds in the Australian lithosphere are in accord with regional studies, and there are some interesting indications of variations in structure in the uppermost mantle.

Simulation of elastic wave propagation using a wavelet transform

T-K Hong and B.L.N. Kennett

Wavelet-based methods in signal processing have been introduced relatively recently, but are already one of the most useful techniques. One of the merits of wavelets is their confined response in both the frequency and time domains and this offers advantages in the field of numerical analysis. In the last few years methods have been developed for solving parabolic partial differential equations (PDEs) in one space dimension and time. This approach has been extended to elastic wave propagation in two space dimensions

In order to adapt the approach developed for a parabolic PDE scheme to the elastic wave equation which is of hyperbolic type, we rewrite the elastic wave equation in a first order PDE system in time in terms of particle velocities and displacements. The spatial differentiation terms are regarded as linear operators which can be represented through a wavelet transform. The forcing terms in the elastic wave equation appears as a non-linear term in the system of first order PDEs. An explicit development in discretised time is made by using a Taylor's series and a semigroup approach to the representation of the linear operators using a hierarchy of wavelets. The representation employs a matrix operator on a vector composed of displacements and velocities. For the case of two space dimensions there is a 2 x 2 matrix operator for SH waves and a 4 x 4 matrix for each of 4 different linear operators in the case of P-SV waves. The wavelet representation provides high order accuracy spatial differentiation and can avoid some of

the problems associated with a staggered-grid scheme in the finite difference method. Higher order accuracy can be introduced in the wavelet representation by increasing the number of terms used in the Taylor expansion with a higher order of spatial differentiation.

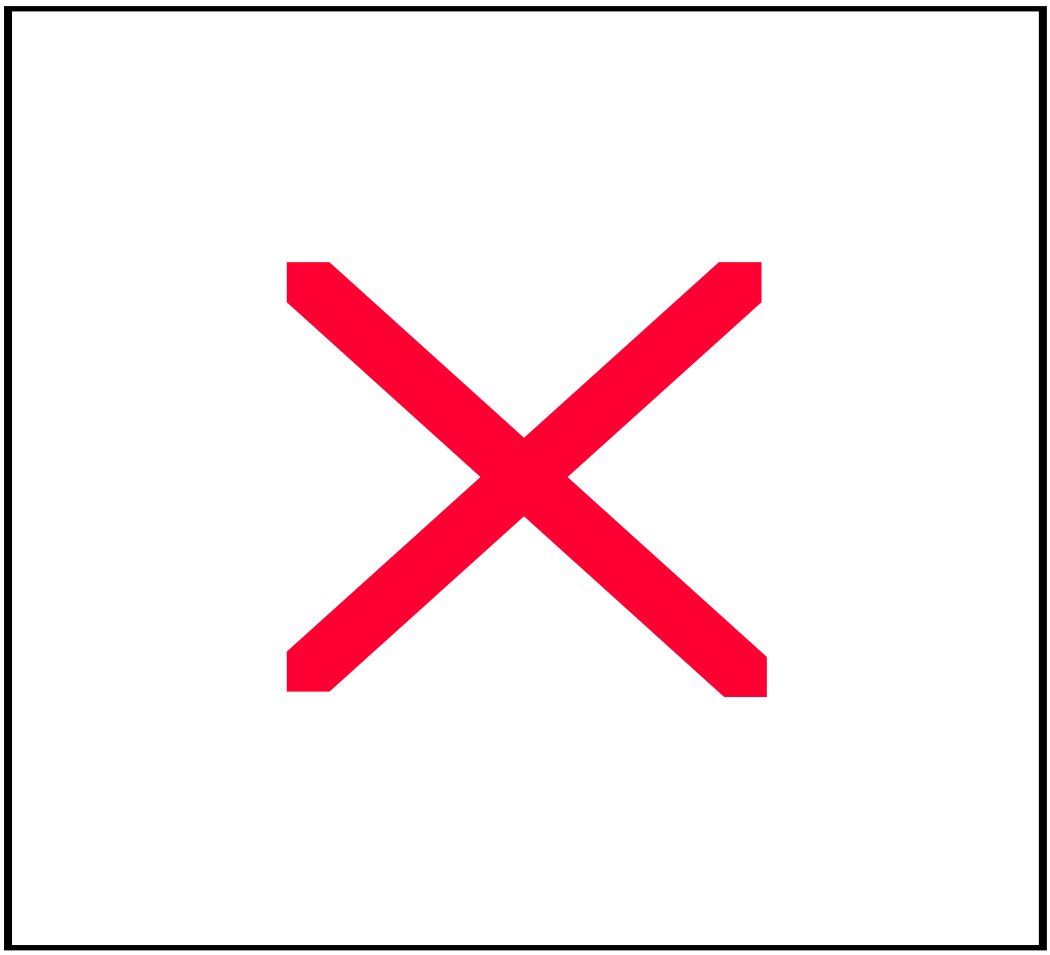

Figure 11: (a) Description of 2D two-layered heterogeneous elastic media. S indicates a source position, the top boundary over the first layer is free surface and the others are absorbing boundaries. (b) SH wave propagation in two-layered heterogeneous media with free surface.

The source is most conveniently introduced by surrounding the source point with a small zone of homogeneous material for which the governing equations are simplified. The source radiation is then passed on to the rest of the computation as a boundary conditions on the perimeter of the homogeneous zone. A damping term is including in the governing equations and is activated near the boundaries of the numerical domain to provide an absorbing bounding condition.

Successful computations have been carried out for both P-SV waves and SH waves in layered and heterogeneous models. The case of SH waves in a two layered model is illustrated by a snapshot of the wavefield in Figure 11, which shows reflection from the free surface as well as reflected and refracted waves from the interface.

Seismogram displays

B.L.N. Kennett

Seismograms are now commonly recorded on 3-orthogonal sensors so that the full vector ground motion can be determined. However, displays of seismograms are still oriented towards single component displays. A number of new display modes have been implemented in the latest version of the ZDF software suite developed at RSES. Various forms of record sections and multi-component displays have been supplemented with a projective display, which can often provide a useful insight into the character of the wavefield. This form of presentation is illustrated in Figure 12(a) for broadband recordings at distances less than 30˚ for an event in southern Xinjiang China. The vertical component seismograms are plotted superimposed on the predicted travel times for the ak135 model which match the observations quite well.

Polarisation displays, based on direct plots of particle motion, are often used to try to convey the three-dimensional motion. An alternative representation is to use summary information for vector behaviour derived by averaging over short time intervals. The evolution of the character of the wavefield can then be conveyed using a triaxial representation of three dimensional motion based on a viewpoint at infinity. The presentation can be based on individual seismograms or in the form of a record section. When combined with a projective display, it is possible to render the change in three-dimensional motion as a function of time as illustrated in the lower panel of Figure 12(b) for the same event as shown in Figure 12(a). The use of colour (or tone) superimposed on the vector representation enables the character of the wavefield to be judged as a function of time; in Figure 12(b) darker tone is used for vertical motion. Figure 12(b) provides a useful complement to the record section in Figure 12(a). The vector displays indicate the presence of a significant S component in the P coda. A change in the polarisation state of the S waves with increasing distance can be also be seen, beyond 20° the SV waves are more prominent (as indicated by the darker tone) and there is noticeable rotation of the polarisation state with time.

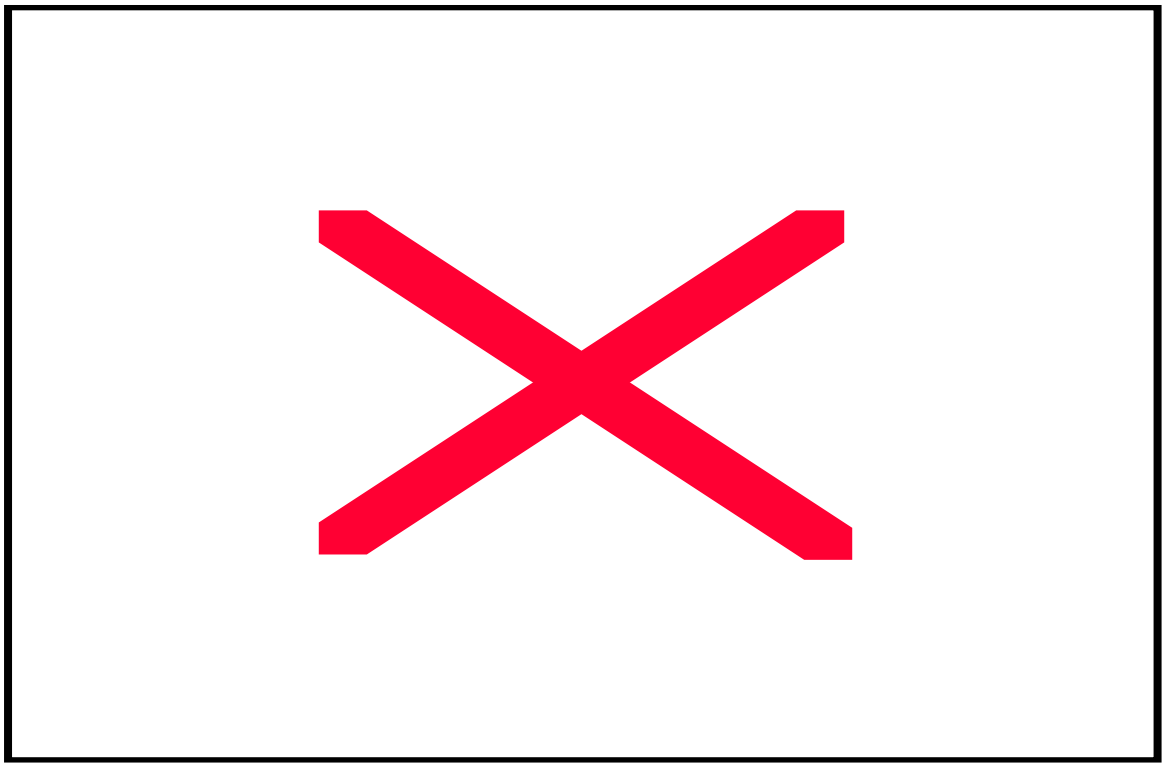

Figure 12: Representation of seismogram behaviour with time for broadband recordings of an event in Xinjiang, China. (a) The vertical component of motion for each station as a function of time in a projective record section. (b) A triaxial representation (u,d - up,down; t,a - towards, away; l,r -left,right) displays the change in vector character as a function of time, the dominant character of the motion is indicated by tone, with lighter tone indicating dominantly horizontal motion.

GEOMAGNETISM

During 2000 collaboration with Flinders University and the University of Adelaide was developed further in carrying out the OCELOT2000 experiment, a marine electromagnetic study of the geological continent-ocean transition off the northwest shelf of Australia. Good progress was made with a further manuscript reporting the PhD work of Dr A.P. Hitchman, and one describing motional induction by ocean currents. The aeromagnetic industry continues to be concerned with the removal of pulsations from offshore magnetic data. The structure causing the Carpentaria conductivity anomaly is coming into good focus, and plans for its further elucidation are being considered.

Following the opening of the RSES new wing, Geomagnetism moved in May to the Jaeger 2 wing of RSES, close to Seismology. In fact, this brought Geomagnetism back into rooms into which it had first moved at the end of 1969, when the Jaeger 2 buildings were new.

Figure 13: Preparation of a seafloor magnetometer for deployment from R.V. Franklin, Indian Ocean, August 2000.

Electromagnetic studies of continental structure

G.S. Heinson[2], A.P. Hitchman, F.E.M. Lilley, P.R. Milligan[3], T. Pedersen, A. White[4]

An ocean–continent electromagnetic transect (termed OCELOT2000) was initiated across the Australian Northwest Shelf. The northwest margin of Australia includes the Pilbara Archaean shield, the Phanerozoic Canning and Carnarvon sedimentary basins, and the Exmouth Plateau. Geophysical measurements of magnetic and electric fields offshore provide a means of

[2] Adelaide University
[3] Australian Geological Survey Organisation
[4] Flinders University

imaging the crust and mantle structure in terms of electrical conductivity. The OCELOT2000 project has two principal aims: the first is to determine the crust-mantle structure and the anisotropy of the continental margin, which links Archaean shield to ocean abyssal plain. The second is to investigate the Canning Basin conductivity anomaly offshore, where it is predicted from land studies to cross the continental margin.

The deployment cruise for the experiment was R.V. Franklin cruise Fr06/00, from Broome to Broome, 2–11 August 2000. Sixteen seafloor MT instruments were deployed in two arrays. Twelve of the instruments were deployed in a linear array across the continental shelf and slope, offshore from the Archaean shield of the Pilbara Block. Another eight sites were occupied by deploying four instruments twice each on the continental shelf, in a line across the predicted Canning Basin anomaly position. The retrieval cruise for the experiment was R.V. Franklin cruise Fr08/00, from Dampier to Dampier, 26–29 September 2000. Analysis of the data recorded is now in progress.

Addressing a different part of the continent, a visit by Associate Professor I.J. Ferguson of the University of Manitoba enabled progress to be made on completing the interpretation of data from the 1997 line of magnetotelluric stations between Julia Creek and Cloncurry in western Queensland. The major electrical conductivity structure (termed the Carpentaria conductivity anomaly) crossed by the line of stations is well-imaged in conductivity sections resulting from two-dimensional inversions.

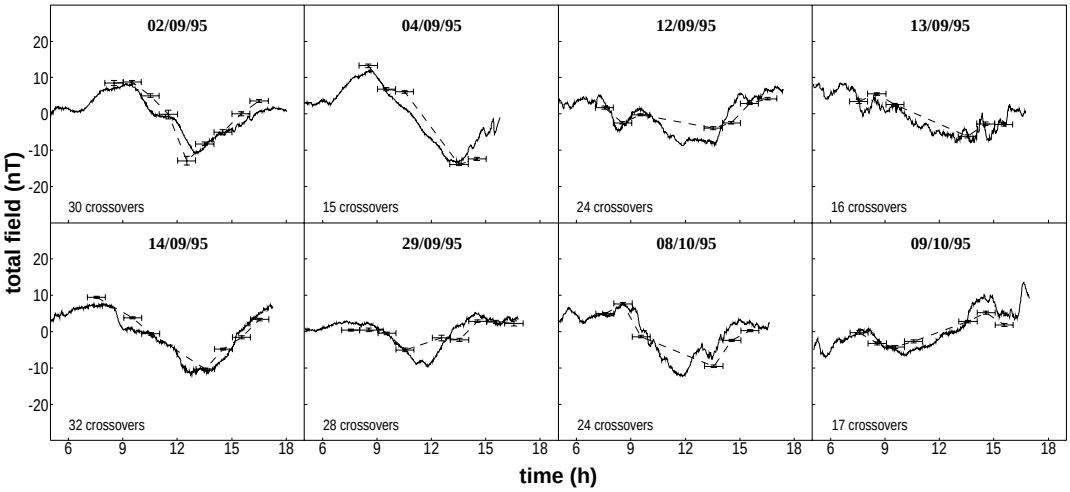

Figure 14: The magnetic daily variation for eight days as recorded by a total-field base-station magnetometer at Broken Hill (shown by continuous lines) compared with diurnal functions recovered from the crossover misfit data of an aeromagnetic survey taking place over the Frome area, several hundred km distant. Crossover misfit data have been put into bins, each of length 1 hour. The results demonstrate the usefulness of crossover misfits as a source of information on the magnetic diurnal variation.

The availability of a great deal of high resolution aeromagnetic data, with accurate navigation and magnetic readings, has stimulated research into the use of cross-over misfits as data for studying electromagnetic induction in the Earth. Aeromagnetic surveys consist both of survey lines and more widely-spaced ties, flown at right angles to the lines. This practice gives rise to crossover points where lines and ties intersect and two separate measurements of the total magnetic field have been made. Differences between such points contains information on electromagnetic induction in the Earth. Methods have been developed to use such data to gain reconnaissance information on regional electrical conductivity structure for an area where an aeromagnetic survey has been carried out.

Figure 14 shows the magnetic daily variation for eight days as recorded by a total-field base-station magnetometer at Broken Hill (shown by continuous lines) compared with diurnal functions recovered from the crossover misfit data of an aeromagnetic survey taking place on

those days over the Frome area, several hundred kilometer distant. Applying these techniques generally to the data of the Frome aeromagnetic survey has demonstrated that the aeromagnetic crossover misfits map the presence of a known electrical conductivity anomaly.

Magnetic and electric fields generated by motional induction

G.S. Heinson[2], A.P. Hitchman, F.E.M. Lilley, T. Pedersen, A. White[4]

The Earth's main magnetic field should have a uniform gradient with depth in the ocean. Superimposed upon this gradient may be signals arising from the motional induction of seawater moving in the steady main magnetic field of Earth. There are circumstances where theory predicts such motionally-induced magnetic fields to be of order 100 nT, and to vary with depth in a way which is directly related to the velocity profile. Exploratory soundings of the magnetic field have been made in the oceans around Australia to test these predictions. The magnetic field parameter observed has been that of the 'total field', which should sense the component of the ocean velocity which lies in the magnetic meridian. The magnetometer has been both lowered by cable from a ship, and also operated free-fall to the seafloor (and return). The three stages of equipment development are shown in Figure 15.

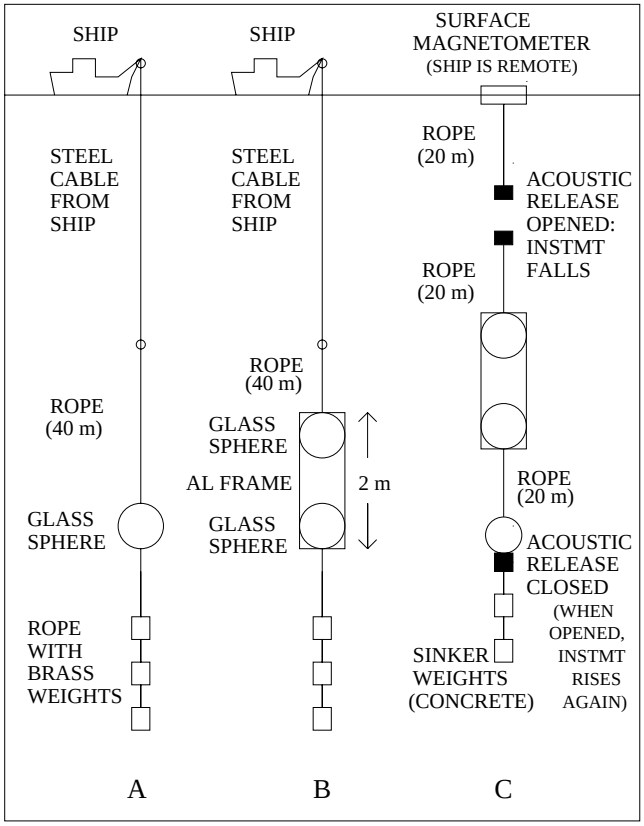

Figure 15: Sketch diagram of the equipment developed for vertical magnetic profiling. Three stages of development are shown as A, B and C, in the progress from a magnetometer completely in a single glass sphere lowered from a ship, to a free-fall and free-rise instrument, in which the magnetometer detector head is separated by a frame from the other magnetometer components. (Note gross changes of scale in different parts of the figure.)

The observations appear both to confirm the theoretical gradient of the main field where there is no ocean current, and where ocean currents exist to give evidence of their profiles resolved in the direction of magnetic north. Especially observations taken in an eddy of the East Australian Current show the correct contrast in sign for north and south flowing streams.

Analysis has been made of data observed by magnetometers which were set to float free on the surface of the ocean, for the purpose of recording the magnetic signals which ocean swells generate by motional induction. The power spectrum of the magnetic signal shows pleasing agreement with predictions from theory. The data are from the Southern Ocean off the coast of South Australia.

Theory

A.K. Agarwal[5], M.R. Ingham[6], F.E.M. Lilley, J.T. Weaver[5]

Work has continued on the optimum method for specifying the seven invariants of a magnetotelluric impedance tensor, especially with a view to clarifying the frequently-encountered case of galvanic distortion. Earlier seven independent rotational invariants of the magnetotelluric impedance tensor were introduced, plus one additional dependent invariant, all of which had a certain physical interpretation when becoming vanishingly small. The seventh independent invariant and the one dependent invariant have now been slightly modified for greater clarity in interpretation, but without affecting their general properties.

Three datasets have been investigated, from Australia, Germany and Canada. The seven invariants have been analysed at each recording site. In those regions where the structure is determined to be regionally two-dimensional, with or without small-scale distortion, the tensor invariants are used to recover a strike angle, as well as the principal impedances.

New electromagnetic induction equipment recently developed at the Victoria University of Wellington, New Zealand, records data according to the 'E-Map' method of magnetotelluric traversing, when the electric field is monitored continously along a traverse across an electrically conductive feature. Computer programs have been developed to support such observations, for both forward modelling, and inversion tasks. The possible application of the method to the detailed investigation of Australian electrical conductivity anomalies has been addressed, especially the Carpentaria anomaly in western Queensland.

[5] University of Victoria, Canada
[6] Victoria University of Wellington